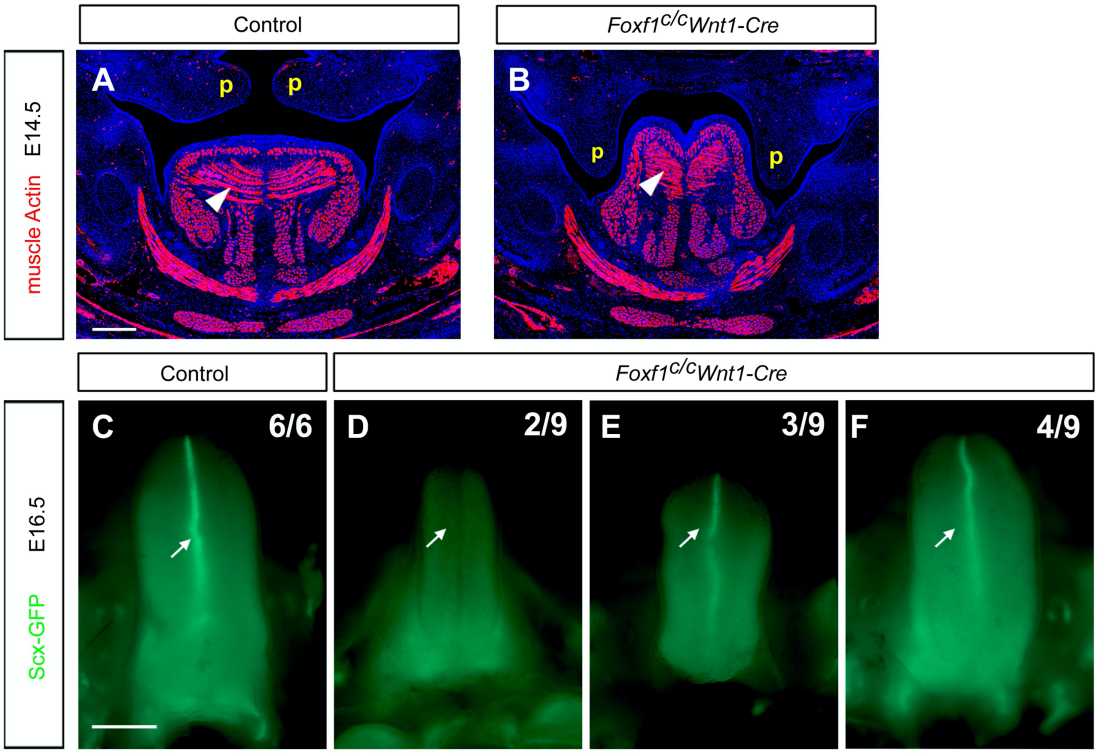

Fig. S1. The *Foxf1*$^{c/c}$*Wnt1-Cre* mutant mice cleft palate and defects in tongue development. (A, B) frontal sections through the tongue of E14.5 control (A) and *Foxf1*$^{c/c}$*Wnt1-Cre* (B) embryos showing immunofluorescent detection of muscle actin (red) (n=3 for each genotype). Arrowhead points to the location of the transverse and vertical muscles in the tongue. p, palatal shelf. (C-F) Whole mount view of E16.5 control (C) (n=6), and *Foxf1*$^{c/c}$*Wnt1-Cre* (D-F) (n=9) embryonic tongue showing the patterns of green fluorescence from the Scx-GFP transgenic reporter. Arrow points to the location of the lingual septum tendon in the tongue. Scale bars: (A, B) 200 μm; (C-F) 1000 μm.

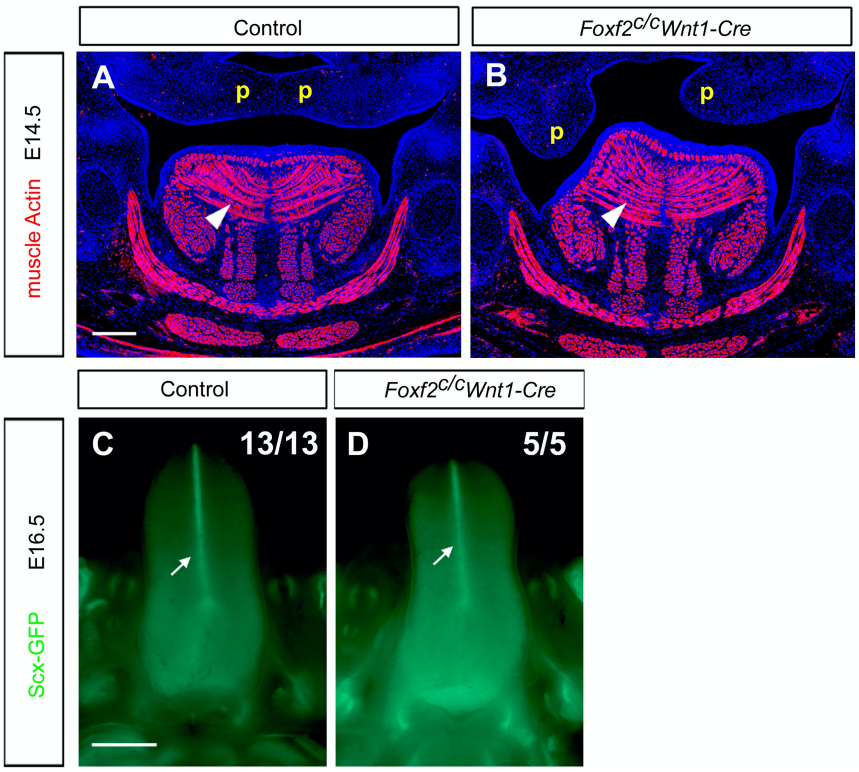

Fig. S2. Palate and tongue phenotype in *Foxf2$^{c/c}$Wnt1-Cre* mice. (A, B) Frontal sections through the tongue of E14.5 control (A), and *Foxf2$^{c/c}$Wnt1-Cre* (B) embryos showing immunofluorescent detection of muscle actin (red) (n=3 for each genotype). Arrowhead points to the location of the transverse and vertical muscles in the tongue. p, palatal shelf. (C, D) Whole mount view of E16.5 control (C) (n=13), and *Foxf2$^{c/c}$Wnt1-Cre* (D) (n=5) embryonic tongue showing the patterns of green fluorescence from Scx-GFP transgenic reporter. Arrow points to the location of the lingual septum tendon in the tongue. Scale bars: (A, B) 200 μm; (C, D) 1000 μm.

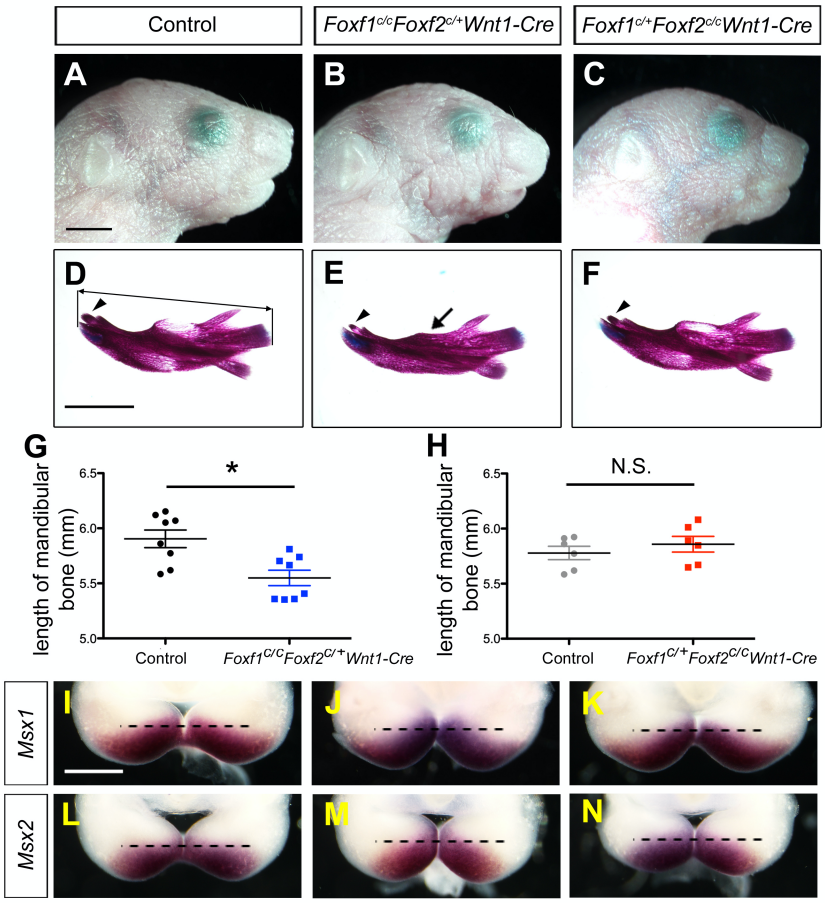

Fig. S3. Craniofacial phenotypes of *Foxf1*$^{c/c}$*Foxf2*$^{c/+}$*Wnt1-Cre* and *Foxf1*$^{c/+}$*Foxf2*$^{c/c}$*Wnt1-Cre* mutant mice. (A-C) Whole mount lateral view of P0 control (A), *Foxf1*$^{c/c}$*Foxf2*$^{c/+}$*Wnt1-Cre* (B), and *Foxf1*$^{c/+}$*Foxf2*$^{c/c}$*Wnt1-Cre* (C) heads (n=3 for each genotype). (D-F) Mandibular bone of P0 control (D), *Foxf1*$^{c/c}$*Foxf2*$^{c/+}$*Wnt1-Cre* (E), and *Foxf1*$^{c/+}$*Foxf2*$^{c/c}$*Wnt1-Cre* (F) mutant embryos. Arrowhead points to the incisor. Arrow in E points to defective molar alveolar bone in the *Foxf1*$^{c/c}$*Foxf2*$^{c/+}$*Wnt1-Cre* embryo. (G, H) Quantitative comparison of the length of the mandibular bone between the control and *Foxf1*$^{c/c}$*Foxf2*$^{c/+}$*Wnt1-Cre* littermates (G) (8 mandibular bones from 4 mice for each genotype) and between control and *Foxf1*$^{c/+}$*Foxf2*$^{c/c}$*Wnt1-Cre* littermates (H) (6 mandibular bones from 3 mice for each genotype). *, $P < 0.05$; N.S., not statistically different. (I-N) Whole mount *in situ* hybridization detection of *Msx1* (I-K) and *Msx2* (L-N) mRNA expression in the mandibular arches in E10.5 control (I, L), *Foxf1*$^{c/c}$*Foxf2*$^{c/+}$*Wnt1-Cre* (J, M), and *Foxf1*$^{c/+}$*Foxf2*$^{c/c}$*Wnt1-Cre* (K, N) embryos. Dashed line crosses the midpoint of the oral-aboral axis at the most distal region of the mandibular arch. Scale bars: (A-F) 2 mm; (I-N) 500 μm.

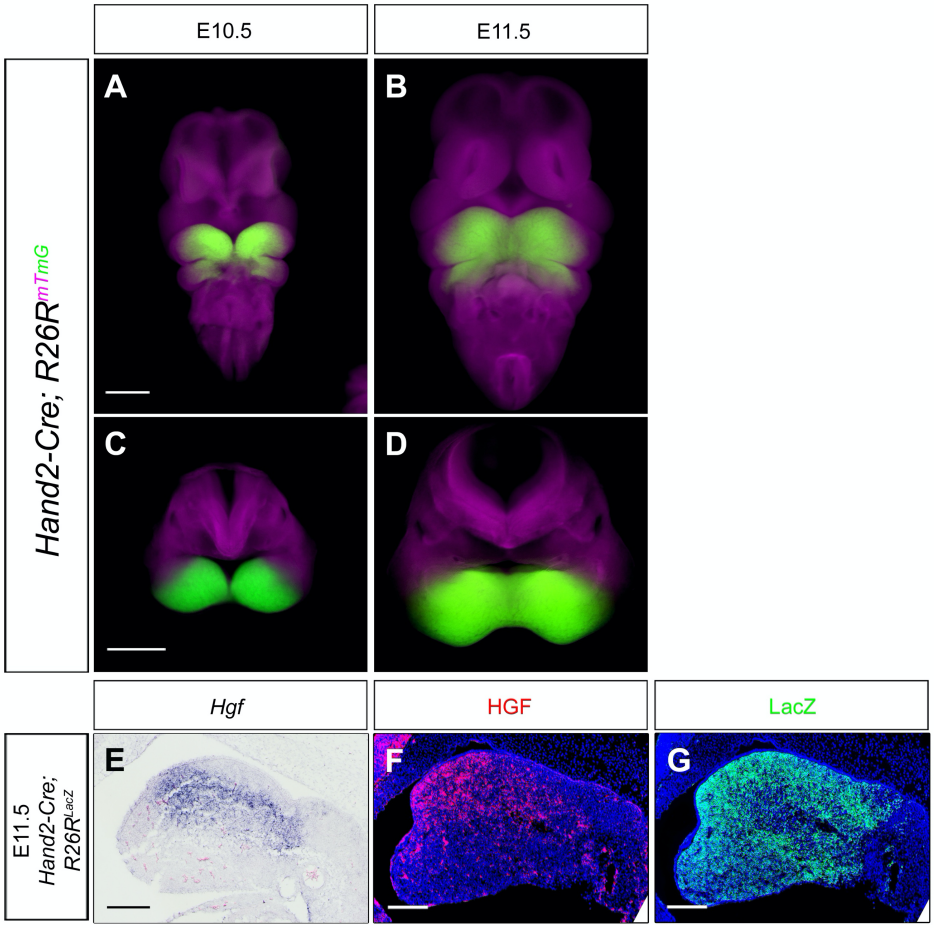

Fig. S4. Hand2-Cre activity and tongue development. (A, B) Whole mount frontal view of E10.5 (A) and E11.5 (B) heads of *Hand2-Cre;R26R*^{mTmG} embryos showing the pattern of GFP (green) and tdTomato (magenta) expressed from the *R26R*^{mTmG} locus. GFP expression marks the Cre lineage cells. (C, D) Whole mount rostral view of dissected mandibular processes from E10.5 (C) and E11.5 (D) *Hand2-Cre;R26R*^{mTmG} embryos showing the patterns of GFP (Green) and tdTomato (magenta). (E-G) Sagittal sections through the tongue and mandible of E11.5 wildtype (E) and *Hand2-Cre;R26R*^{LacZ} (F, G) embryos showing patterns of *Hgf* mRNAs (E, blue) and immunofluorescent staining of HGF protein (F, red) and LacZ protein (G, green), respectively. LacZ expression from the *R26R*^{LacZ} locus marks the Cre lineage cells. Scale bars: (A-D) 1000 μm; (E-G) 200 μm.

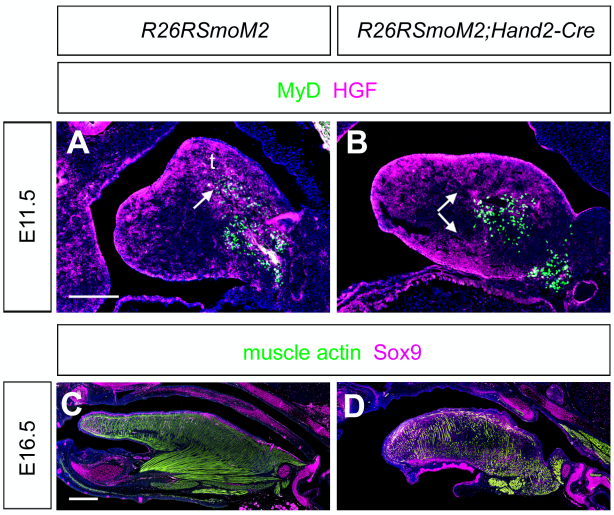

Fig. S5. Hedgehog signaling regulates tongue myogenesis through controlling the expression of HGF during early tongue development. (A, B) Sagittal sections of E11.5 *R26RSmoM2* control (A) and *R26RSmoM2;Hand2-Cre* (B) embryos showing patterns of immunofluorescent staining of HGF (magenta) and MyoD. Arrows point to the expression of HGF protein. (C, D) Sagittal sections through the developing mandible and tongue of E16.5 *R26RSmoM2* control (C) and *R26RSmoM2;Hand2-Cre* (D) embryos showing patterns of immunofluorescent staining of Sox9 (magenta) and muscle actin (green). Scale bars: 200 μm in (A, B), 500 μm in (C, D).

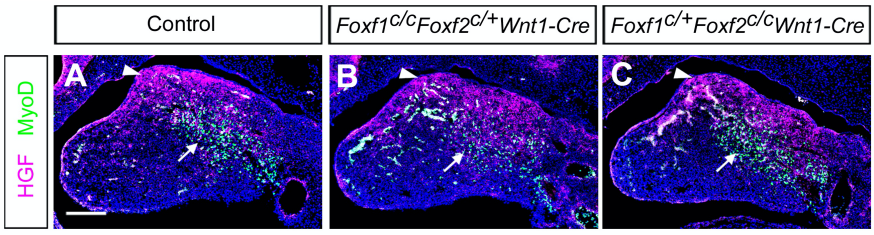

Fig. S6. Patterns of HGF and MyoD expression during initial tongue formation in *Foxf1$^{c/c}$Foxf2$^{c/+}$Wnt1-Cre* and *Foxf1$^{c/+}$Foxf2$^{c/c}$Wnt1-Cre* embryos. (A-C) Sagittal sections through the developing tongue and mandible of E11.5 control (A), *Foxf1$^{c/c}$Foxf2$^{c/+}$Wnt1-Cre* (B), and *Foxf1$^{c/+}$Foxf2$^{c/c}$Wnt1-Cre* (C) embryos showing patterns of immunofluorescent staining of HGF (magenta) and MyoD (green) (n=3 for each genotype). Arrowhead points to the anterior tip of the tongue primordium. Arrow points to the myogenic progenitor cells. Scale bars: (A-C) 200 μm.